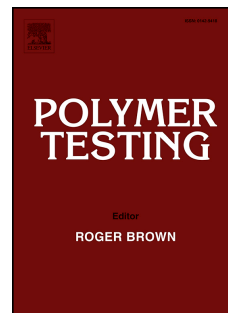


# Accepted Manuscript

Effect of processing on the environmental stress cracking resistance of high-impact polystyrene

Luca Andena, Marta Rink, Claudia Marano, Francesco Briatico-Vangosa, Leonardo Castellani



PII: S0142-9418(16)30364-6

DOI: [10.1016/j.polymeresting.2016.06.017](https://doi.org/10.1016/j.polymeresting.2016.06.017)

Reference: POTE 4690

To appear in: *Polymer Testing*

Received Date: 20 April 2016

Accepted Date: 18 June 2016

Please cite this article as: L. Andena, M. Rink, C. Marano, F. Briatico-Vangosa, L. Castellani, Effect of processing on the environmental stress cracking resistance of high-impact polystyrene, *Polymer Testing* (2016), doi: 10.1016/j.polymeresting.2016.06.017.

This is a PDF file of an unedited manuscript that has been accepted for publication. As a service to our customers we are providing this early version of the manuscript. The manuscript will undergo copyediting, typesetting, and review of the resulting proof before it is published in its final form. Please note that during the production process errors may be discovered which could affect the content, and all legal disclaimers that apply to the journal pertain.

## Effect of processing on the environmental stress cracking resistance of high-impact polystyrene

Luca Andena<sup>a,\*</sup>, Marta Rink<sup>a</sup>, Claudia Marano<sup>a</sup>, Francesco Briatico-Vangosa<sup>a</sup>, Leonardo Castellani<sup>b</sup>

<sup>a</sup> Politecnico di Milano, Dipartimento di Chimica, Materiali e Ingegneria Chimica “Giulio Natta”, Piazza L. Da Vinci, 32, Milano (Italy)

<sup>b</sup> Versalis SpA, Basic Chemicals & Plastics Research Center, Via G. Taliercio, 14, Mantova (Italy)

\* corresponding author ([luca.andena@polimi.it](mailto:luca.andena@polimi.it); tel +390223993289)

### Abstract

Processing conditions have a strong effect on the final mechanical properties of products made of polymeric materials. Relevant phenomena most commonly include thermal stresses, physical ageing, frozen-in strains and molecular orientation. In this work, two different high-impact polystyrenes, processed by thermoforming, were considered: a “standard” one and a grade specifically resistant to Environmental Stress Cracking (ESC). The main effect induced by thermoforming was molecular orientation. The local degree of orientation was measured on a thermoformed product and its effect on the material ESC behavior in sunflower oil was studied. A Fracture Mechanics approach was applied to evaluate the fracture resistance of the two materials. Results show that a higher degree of orientation increases the fracture resistance in air but has no effect on the (expectedly lower) resistance in the active oil environment.

### Keywords

Polystyrene; Environmental Stress Cracking; Processing; Fracture

## 1. Introduction

Polymeric materials in the form of powder or pellets can be shaped to obtain products following a complex thermo-mechanical processing history. This history strongly influences many different properties of the constituent material and, consequently, the products' actual performance. According to Struik [1], the main effects of processing are: (i) physical ageing, which is the consequence of the viscoelastic volume relaxation towards equilibrium experienced by polymers cooled below their glass transition temperature,  $T_g$ ; (ii) residual thermal stresses, which originate from temperature gradients in the product when more or less rapidly cooled from the high temperatures necessary for shaping; (iii) residual strains, due to the viscoelastic nature of polymeric materials which retain memory of the stresses applied during processing; (iv) molecular orientation, induced by viscous flow at high temperatures, which becomes frozen-in during cooling. In the case of semicrystalline materials, the degree of crystallinity and the specific orientation of the crystalline phase could also be influenced by the processing conditions. All these variables exert a strong effect on the mechanical characteristics of the final products.

ESC is a well-known phenomenon by which the presence of certain substances facilitates initiation and growth of fracture in a given material, effectively reducing the levels of applied stress necessary for its occurrence [2-5]. In the presence of the said substances, even small residual stresses – otherwise unharmed – may trigger fracture and lead to the premature failure of a component.

In this research, the two themes of processing and ESC were put together. There are only a handful of studies regarding the effects of processing on ESC resistance, and often a single effect is considered: examples can be found in [6-7] for orientation on high impact polystyrene (HIPS) and crystallinity on polyethylene, respectively.

The material investigated in this work was HIPS, for which food oils are known ESC-promoting agents [2,6]. Firstly, the effects of the thermoforming process on a HIPS thermoformed product were analyzed, ascertaining their presence and their spatial distribution. In a second stage, samples were obtained directly from the thermoformed product and the material's fracture resistance was evaluated using the fracture mechanics (FM) approach, which has been previously applied by the authors to study the resistance of different polymers to Environmental Stress Cracking (ESC) [2-3], to obtain a correlation between processing effects and ESC resistance.

## 2. Materials

Two different HIPS (named A and B), previously studied in [2], were investigated. HIPS-A and HIPS-B are a specifically ESC resistant and a standard grade, respectively; the former exhibits a significantly higher resistance to ESC in sunflower oil environment. ESC resistance measured with the bent strip test (ISO 22088-3 at 0.5% def. – 50 min–23 °C) gives  $\varepsilon_r/\varepsilon_0\%$  of 94 and 26 for HIPS-A and HIPS-B, respectively.

Mechanical properties (elastic modulus, yield stress, impact resistance) in air are quite similar for the two materials. Some differences are due to a larger (by about 10%) dispersed phase content for HIPS-A, which also has a larger average rubber particle size.

The two materials were supplied by Versalis SpA in the form of pellets, extruded sheets (about 4 mm thick) and a thermoformed laboratory product. Pellets were compression molded into 200x170 mm plates with thicknesses of 1.5 and 4 mm. The thermoformed product studied is shown schematically in Figure 1, together with its relevant dimensions and the parts (1-5) which were cut out to test. This product, obtained starting from an extruded sheet, has an average thickness of about 1.5 mm.

### 3. Evaluation of processing effects

As already mentioned in the introduction, four main effects of processing may be expected. Their relative importance depends on the particular processing conditions adopted. According to the nature of each one, they were investigated on the thermoformed laboratory product and/or the extruded sheets by tracking dimensional changes following different thermal treatments, with the exception of physical ageing the presence of which was detected by performing tensile tests. Measurements of dimensional changes of parts 1-5 cut from the thermoformed product were performed by aid of a stamped ink grid with a square pattern. As an example, Figure 2 shows two pictures of part 3 of the HIPS-B thermoformed product, taken before and after one of the thermal treatments.

#### *Physical ageing*

Polymeric glasses are in a non-equilibrium volumetric state; this in turn depends on the thermal history experienced by the polymer while cooling from processing to room temperatures, as well as on the amount of time elapsing thereafter, since volume evolves towards equilibrium. The effects of these volumetric changes are called physical ageing. Several mechanical properties depend on the actual volumetric state; in this work, tensile yield stress has been considered. Yield stress has been determined as the maximum in the stress-strain curves, being aware that at this value multiple crazing occurs in HIPS. It was measured on samples cut from extruded sheets (kept for several weeks at 23°C), before and after a 1h thermal treatment at 90°C, which is just below the glass transition temperature of the polystyrene matrix of HIPS ( $T_g \approx 100^\circ\text{C}$ ), followed by a fast cooling in air to 23°C. Because this thermal treatment should rejuvenate the material, the samples before and after the treatment will be referred to as “aged” and “un-aged samples” respectively.

Tensile tests were then performed at 23°C on an Instron 1121 electro-mechanical dynamometer with a constant crosshead speed of 1 mm/min; strains were measured using a mechanical extensometer. Samples geometry and dimensions are shown in Figure 3.

#### *Thermal stresses*

Thermal stresses are caused by temperature gradients present across the thickness of the product during cooling through the glass transition temperature. They can be removed by annealing the product close or at  $T_g$  and then slowly cooling it down to room temperature. Generally, unless the thermal stress distribution is perfectly symmetric across the thickness, the product considered will distort after such a thermal treatment. The presence of such warping was searched for after performing thermal treatment at 90°C for 1h, followed by slow cooling to 23°C.

#### *Residual strains*

Residual strains depend on the stress level in the product during cooling through the glass transition. They can be recovered by annealing the material to a temperature close to  $T_g$ ; a dimensional change is expected in this case. This was checked by carefully measuring the samples before and after applying the same treatment considered for removing thermal stresses.

#### *Molecular orientation*

Molecular orientation is the consequence of frozen-in non-equilibrium conformations. It is originated by high stresses applied during product shaping above  $T_g$  and it becomes, subsequently, frozen-in during fast cooling. Molecular orientation requires annealing treatment above the glass transition temperature to be removed. Again, dimensional changes are expected if orientation is removed and the method chosen to check their presence takes advantage of this fact. A thermal treatment for 1 hour at 140°C was applied to the samples, followed by slow cooling to room

temperature; subsequent dimensional changes with respect to the original dimensions were measured by defining a suitable orientation index,  $O$ , as the opposite of the apparent strain calculated according to Equation 1:

$$O = -\frac{\Delta L}{L_0} \quad (1)$$

in which  $\Delta L$  is the variation in the distance between two grid marks originally (i.e. before the thermal treatment) at a distance  $L_0$ . A positive value of the orientation index indicates that there is molecular orientation in the direction along which  $\Delta L$  was measured.

#### 4. Fracture tests

FM was considered in its most simple formulation, Linear Elastic Fracture Mechanics (LEFM) [8], following which the stress intensity factor,  $K_I$ , completely characterizes the stress field around a sharp crack tip and, as a consequence, fracture will initiate from a given defect (or sharp notch) when  $K_I$  exceeds a critical value,  $K_{IC}$ , which is the material's fracture toughness. The subscript "I" refers to opening fracture mode. Fracture tests were carried out at 23°C with an Instron 1121 electromechanical dynamometer at constant nominal strain rate of  $4.2 \cdot 10^{-5} \text{ s}^{-1}$  on double and single edge notched specimens in tension referred to as DEN(T) and SEN(T), respectively; their dimensions are shown in Figure 4. Notches were introduced into the specimens by razor broaching, checking that the resulting notch root radius was smaller than 10  $\mu\text{m}$ . The tests in a sunflower oil environment were performed using a custom-designed bath [2] fitted with inspection windows.

Continuous video recording was conducted using an IDS UI-1480LE digital camera to measure crack length. Occasionally, extensive crack blunting prevented a reliable identification of crack onset by visual observation: for this reason fracture initiation time,  $t_i$ , was conventionally

determined by the time at which the crack length vs. time curve exceeded its initial value by 5%. In a previous paper [2], in which the same fracture mechanics approach was adopted, it was shown that a time of about 100s is necessary for the sunflower oil to interact with the HIPS in a notched test. Thus, the displacement rate was chosen so as to have initiation times for fracture always longer than 100s.

From the relevant load at  $t_i$  the critical stress intensity factor at fracture initiation,  $K_{IC}$ , was determined according to Equation 2:

$$K_{IC} = Y \cdot \sigma_C \cdot \sqrt{\pi a} \quad (2)$$

with  $\sigma_C$  being the global stress at crack onset,  $a$  the initial notch length and  $Y$  a shape factor whose value was obtained according to [10].

To verify that  $K_{IC}$  is indeed independent of the actual testing configuration and specimen geometry, preliminary tests in air on different DEN(T) and SEN(T) samples obtained from the compression molded sheets of HIPS-B were first carried out. It was found that the two configurations gave identical results for both thicknesses considered (1.5 and 4mm). On the other hand, a noticeable effect was observed while varying the ligament length: in particular, a lower apparent value of toughness was measured for samples having an uncracked (initial) ligament length lower than 15mm, as shown in Figure 5. Too small a ligament length hinders the full development of the plastic zone around the crack tip, and thus reducing the fracture resistance. A similar effect has been previously reported for other polymeric materials [11-12]. To avoid the need for samples of excessive size – in view of making them out of the thermoformed product – the use of SEN(T) configuration was preferred.

## 5. Results and discussion

### 5.1 Processing effects

#### *Physical ageing*

No significant difference between the yield stress of aged and unaged samples was found, as shown in Table 1 for both HIPS-A and HIPS-B. It is known that physical aging for polystyrene at room

temperature is limited and, therefore, a significant difference in volumetric state would arise only in samples subjected to very different cooling rates; results suggest that this was not the case in the investigated conditions.

#### *Thermal stresses*

No sign of distortion after the thermal treatment was observed for the extruded sheets. Minor distortions were observed only in some parts of the thermoformed product made of HIPS-A. Overall, thermal stresses seemed to play a very minor role for the case under investigation and, accordingly, they were not considered further.

#### *Residual strains*

No dimensional change was observed after performing the thermal treatment neither in the extruded sheets nor in the thermoformed products. Therefore, residual strains appear to be negligible.

#### *Molecular orientation*

Dimensional changes were observed after the thermal treatment both in the thermoformed product parts and the extruded sheets. A map of the orientation index in the two perpendicular in-plane directions for each part of the thermoformed product was obtained for HIPS-B: they are depicted in figures 6-10. Depending on the relevant part size, two or four grids were considered for each. It can be observed that the orientation varies considerably in the different parts.

In the case of HIPS-A, mapping of parts 1, 2 and 5 could not be performed because they rolled up after annealing, as shown in Figure 11. This is most likely due to a different orientation level on the internal and external surfaces of the thermoformed product. The orientation maps of parts 3-4 were qualitatively similar to those of HIPS-B.

As expected, the orientation level is high in the z direction, which corresponds to the drawing direction during thermoforming, while it is low or even negative in the transverse direction. A detailed analysis of the orientation and of its correlation with the specific thermoforming process is beyond the scope of this work. However, it is useful to observe areas showing a constant level of orientation, from which specimen for the mechanical characterization could be cut.

As for the extruded sheets, orientation was found to be uniform in the sheets and identical for the two materials (HIPS-A and HIPS-B). Relevant results are listed in Table 2.

## 5.2 Fracture

The data obtained from compression molded sheets, extruded sheets and thermoformed products were compared in terms of the critical stress intensity factor. The study was mainly performed on HIPS-B, for which all thermoformed parts were available; a few samples of HIPS-A were also tested for comparison purposes. Figure 12 reports, for tests performed in air and sunflower oil,  $K_{IC}$  as a function of the orientation index,  $O$ , measured in the direction perpendicular to the notch plane (corresponding to that of the opening stress). In the case of specimens cut from the thermoformed products, the value of  $O$  from the orientation map at the position of the notch tip was used. For the extruded material, the orientation index reported in table 2 value were considered, while for the compression molded sheets a value of  $O$  equal to zero was assumed.

In air, both materials (HIPS-A and HIPS-B) show an increase in fracture toughness with increasing orientation in the direction perpendicular to the crack; in particular, fracture resistance of HIPS-B is larger than HIPS-A at all orientations examined. A significant reduction of  $K_{IC}$  occurs for fracture in sunflower oil, as expected; the envisaged higher resistance of HIPS-A to ESC only becomes evident for values of applied  $K$  much lower than those applied in the present work, as already discussed in

[2]. Besides the obvious reduction of toughness in the presence of oil, a noticeable reduction in the sensitivity to orientation can be observed, especially in the case of HIPS-B, for which the value of  $K_{IC}$  is fairly independent of  $O$  on a relatively large set of data.

These results can be explained by considering a change in fracture propagation mechanism for the more oriented samples when tested in sunflower oil. While in all the other cases crack growth occurs, as expected, along the notch plane direction, crack deviation was observed at high levels of orientation and in the presence of the active environment. The two distinct forms of fracture are shown in Figure 13 in the case of HIPS-B (the same effect was also observed on HIPS-A): forward crack propagation for low orientation and crack deviation for high orientation. When crack deviation takes place, the dependence of toughness on material orientation is suppressed, as previously mentioned. Crack deviation from the notch plane has been already reported by other authors [13-14] who related it to the interaction between stress triaxiality induced at the crack tip and a sufficient degree of fracture resistance anisotropy possessed by the material, causing sideways crack propagation to become energetically favourable.

The dependence of toughness on orientation (in air) is consistent with such anisotropy: the oriented molecular chains hinder the development of a crack crossing them with respect to what happens in the un-oriented material. This strength anisotropy increases in the presence of oil: the stress cracking agent is more likely to influence the intermolecular interactions rather than the covalent bonds along the chain. For this reason, a larger reduction in fracture resistance is expected in the direction parallel to material orientation, to the point that crack propagation more favourably occurs in a direction not along the notch plane.

## 6. Conclusions

Effects of processing thermo-mechanical history were assessed on two different HIPS by investigating samples obtained from compression molded and extruded sheets and a thermoformed laboratory product. In particular, the effects on the resistance to ESC were investigated using a fracture mechanics approach.

For both materials, it was found that the main effect induced by extrusion and thermoforming was molecular orientation, while other possible consequences of processing (physical ageing, thermal stresses, residual strains) were not as significant. Molecular orientation was found to affect crack development in air, with an increase in fracture resistance when the orientation occurs in the direction perpendicular to the crack plane.

As expected, a noticeable reduction of fracture toughness was observed when the two HIPS were tested in a known ESC agent such as sunflower oil. A less obvious effect of the active agent is the suppression of the dependence on molecular orientation (more evident for one of the two materials investigated) which has been related to the different interaction with regard to intra- or inter-molecular bonds. The ESC agent intensifies the orientation-induced material strength anisotropy to the point that a change in fracture mechanism is observed, with the crack deviating from the original notch plane.

This study highlights the need for an increased awareness of the effects of processing on the final products' properties. Most products are currently designed assuming material properties which are obtained on laboratory samples – which may significantly differ from the real ones. Ideally, process-related aspects should be considered to prevent unexpected failures and to optimize process variables, possibly improving the actual performance of final products.

## Acknowledgements

The authors wish to thank Margherita Pecoraro and Francisco Sacchetti for carrying out the experiments and Oscar Bressan for preparing the samples.

## References

1. L.C.E. Struik. Internal Stresses, Dimensional Instabilities and Molecular Orientations in Plastics, 1st ed. John Wiley & Sons. 1990
2. L. Andena, L. Castellani, A. Castiglioni, A. Mendogni, M. Rink, F. Sacchetti. Determination of environmental stress cracking resistance of polymers: Effects of loading history and testing configuration. *Eng Fract Mech* 2013;101:33.
3. L. Andena, L. Castellani, A. Castiglioni, A. Mendogni, M. Rink, F. Sacchetti, A. Adib In: Proceedings of the 15th International Conference on Deformation, Yield and Fracture of Polymers, Rolduc Abbey, Kerkrade, 2012. p. 182-185.
4. J.A. Jansen. Plastic Component Failure Analysis. *Adv Mater Process* 2004;162:50.
5. D.S.A. De Focatiis, C.P. Buckley. Determination of craze initiation stress in very small polymer specimens. *Polym Test*. 2008;27: 136.
6. V. Altstaedt, S. Keiter, M. Renner, A. Schlarb. Environmental stress cracking of polymers monitored by fatigue crack growth experiments. *Macromol Symp* 2004;214:31.
7. A. Sharif, N. Mohammadi, S.R. Ghaffarian. Practical work of crack growth and environmental stress cracking resistance of semicrystalline polymers. *J Appl Polym Sci* 2009;112:3249.
8. L. Andena, M. Rink, F. Polastri. Simulation of PTFE sintering: thermal stresses and deformation behavior. *Polym Eng Sci* 2004;44:1368.

9. T.L. Anderson. Fracture Mechanics: Fundamentals and Applications, 2nd ed. CRC Press 1994
10. D.P. Rooke, D.J. Cartwright. Compendium of Stress Intensity Factors, 1st ed. H.M. Stationary 1976
11. L. Andena, R. Frassine, M. Rink, M. Roncelli In: Proceedings of the 4th International Conference on the Fracture of Polymers, Composites and Adhesives, Les Diablerets, 2005. p. P01.
12. S. Hashemi, J.G. Williams. Size and loading mode effects in fracture toughness testing of polymers. J Mat Sci 1984;19:3746.
13. A.N. Gent, M. Razzaghi-Kashani, G.R. Hamed. Why Do Cracks Turn Sideways?. Rubber Chem Technol 2003;76:122.
14. K. Kendall. Transition between cohesive and interfacial failure in a laminate. Proc R Soc Lond A 1972;344:287.

## Figure Captions

Figure 1. Schematic of thermoformed product considered, with cut out parts 1-5 indicated (dimensions are in mm).

Figure 2. Part 3 of thermoformed product, before and after the thermal treatment (TT: 1h at 90°C). The corresponding grid geometry distortion is visible.

Figure 3. Geometry of the sample used for tensile tests (dimensions are in mm).

Figure 4. In-plane dimensions of the samples used for fracture tests. The value of  $H$  refers to the gauge length, with the samples actually being longer to allow for firm gripping.

Figure 5. Fracture toughness  $K_{IC}$  of HIPS-B as a function of (initial) ligament length for DEN(T) and SEN(T) samples obtained from compression molded sheets. The dashed line represents the average value of  $K_{IC}$  calculated for values of ligament length larger than 15mm.

Figure 6. Orientation map of upper and lower sections of Part 1 of HIPS-B. The orientation index,  $O$ , is plotted as percent value for the z (left) and x (right) direction, according to the coordinate system indicated in Figure 1.

Figure 7. Orientation map of the four sections of Part 2 of HIPS-B. The orientation index,  $O$ , is plotted as percent value for the z (a) and y (b) direction, according to the coordinate system indicated in Figure 1.

Figure 8. Orientation map of upper and lower sections of Part 3 of HIPS-B. The orientation index,  $O$ , is plotted as percent value for the z (left) and y (right) direction, according to the coordinate system indicated in Figure 1.

Figure 9. Orientation map of front and back sections of Part 4 of HIPS-B. The orientation index,  $O$ , is plotted as percent value for the x (left) and y (right) direction, according to the coordinate system indicated in Figure 1.

Figure 10. Orientation map of upper and lower sections of Part 5 of HIPS-B. The orientation index,  $O$ , is plotted as percent value for the z (left) and x (right) direction, according to the coordinate system indicated in Figure 1.

Figure 11. Parts 1, 2 and 5 of thermoformed product made of HIPS-A after thermal treatment at  $T > T_g$ .

Figure 12. Fracture toughness,  $K_{IC}$ , as a function of orientation index in the direction perpendicular to the notch plane. Data obtained in air and sunflower oil, on specimens cut from compression molded sheets, extruded sheets and thermoformed products.

Figure 13. Fracture phenomenology of HIPS-B in air and sunflower oil, respectively for low (left) and high (right) orientation. The sequences of images are taken at different stages during the fracture test: initially and before, at and after the initiation time,  $t_i$ . The dashed lines represent the initial crack tip position.

Table 1. Tensile yield stress  $\sigma_y$  of samples obtained from extruded sheets, before and after an annealing treatment of 1h at 90°C. Data represent the average of four samples for each condition.

Yield stress (MPa)		
	HIPS-A	HIPS-B
aged (before TT)	10.18±0.47	15.09±0.20
unaged (after TT)	10.84±0.20	15.24±0.11

Table 2. Orientation index of extruded sheets

<b>Direction</b>	<b>Orientation index (O)</b>
Extrusion	12%
Transverse	-4%

ACCEPTED MANUSCRIPT

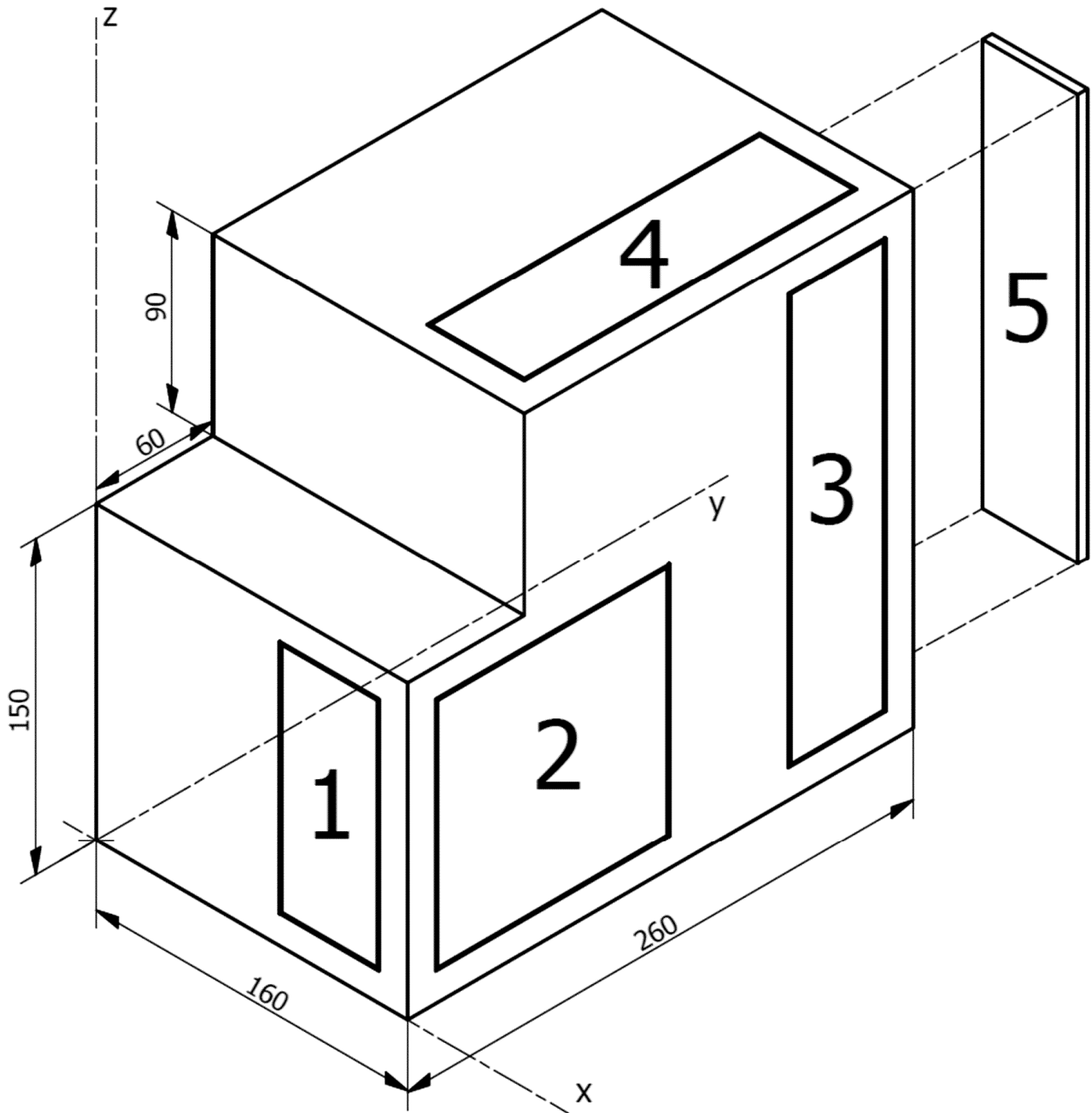


Figure 1. Schematic of thermoformed product considered, with cut out parts 1-5 indicated (dimensions are in mm).

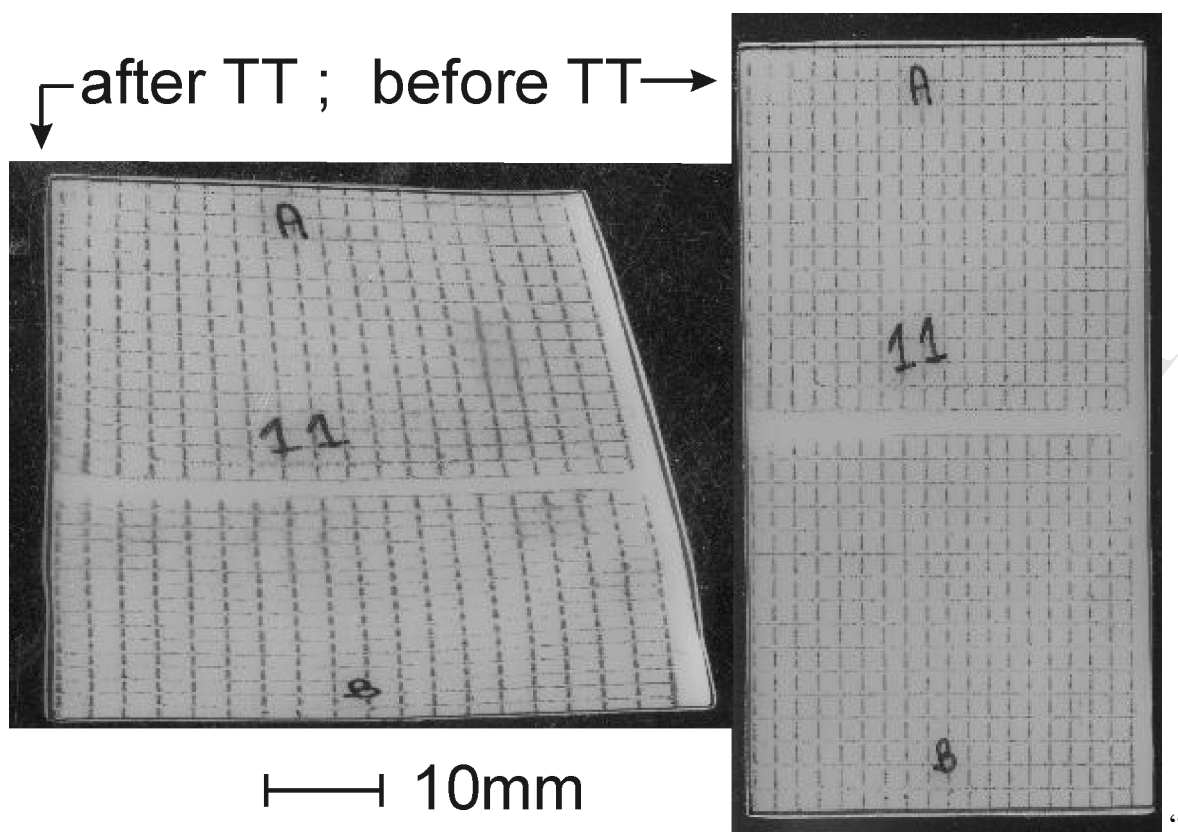


Figure 2. Part 3 of thermoformed product, before and after the thermal treatment (TT: 1h at 90°C). The corresponding grid geometry distortion is visible.

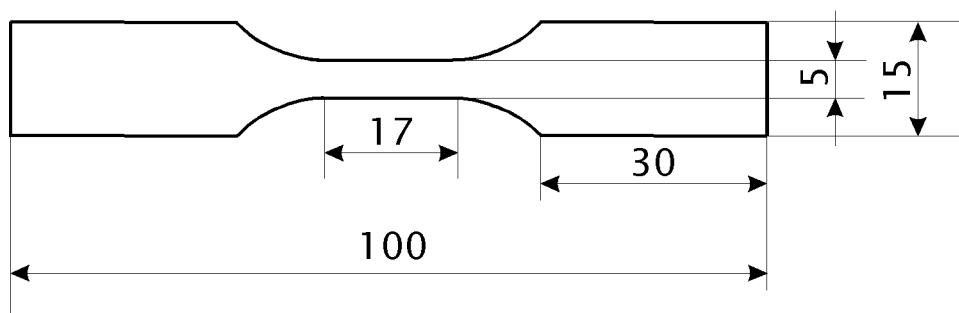


Figure 3. Geometry of the sample used for tensile tests (dimensions are in mm).

ACCEPTED MANUSCRIPT

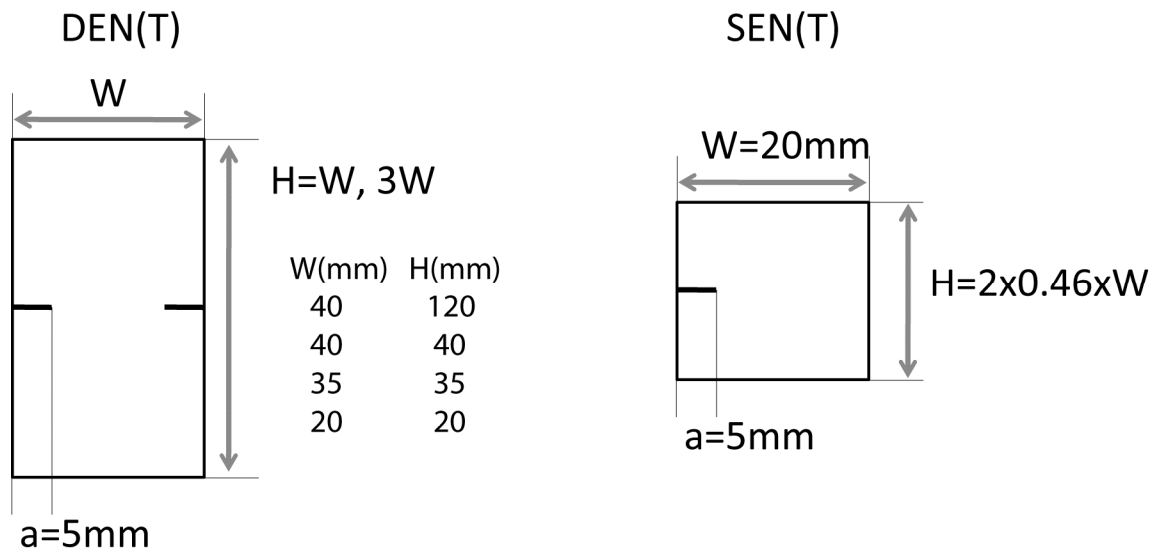


Figure 4. In-plane dimensions of the samples used for fracture tests. The value of  $H$  refers to the gauge length, with the samples being longer to allow for firm gripping.

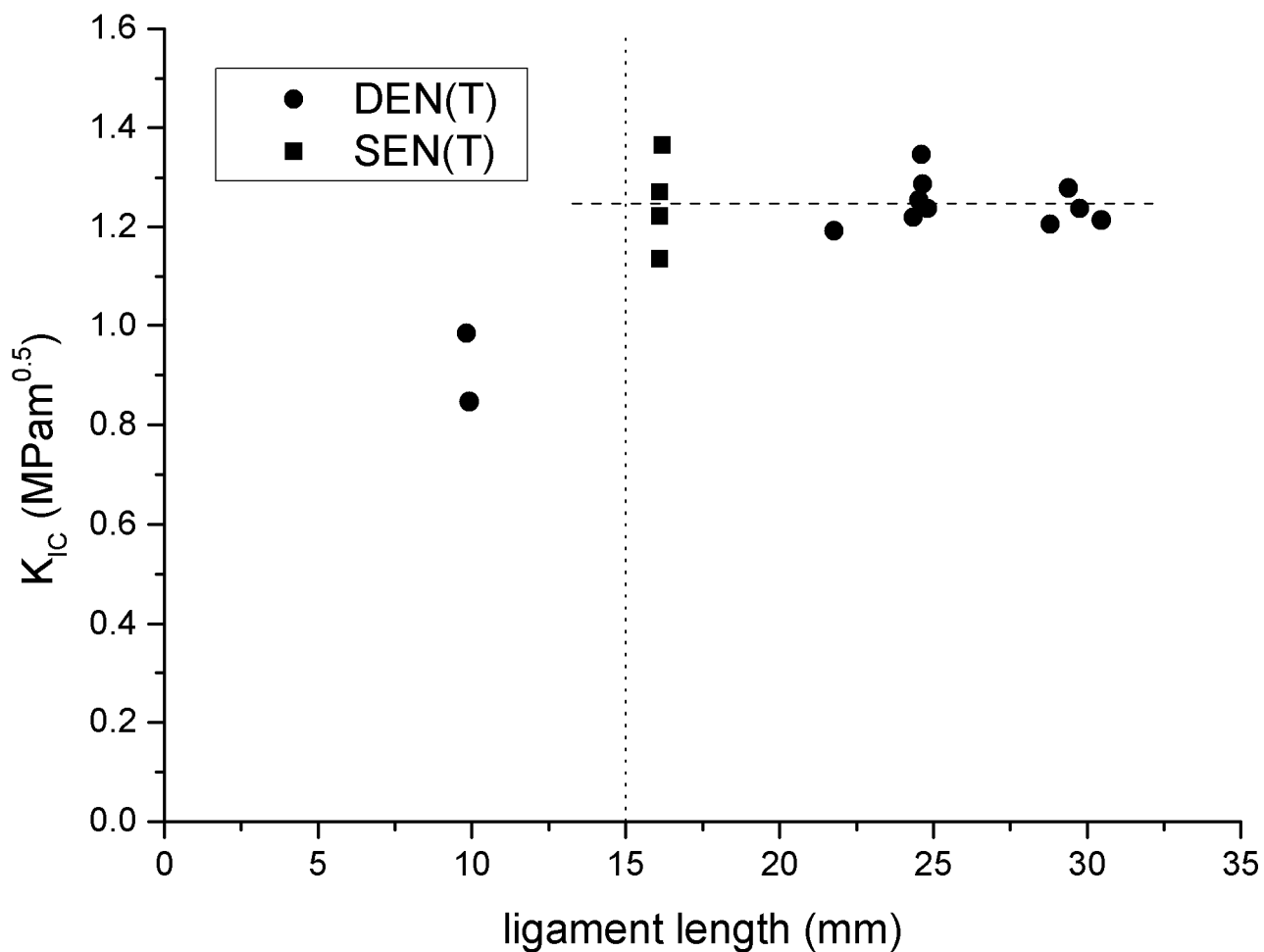


Figure 5. Fracture toughness  $K_{IC}$  of HIPS-B as a function of (initial) ligament length for DEN(T) and SEN(T) samples obtained from compression molded sheets. The dashed line represents the average value of  $K_{IC}$  calculated for values of ligament length larger than 15mm.

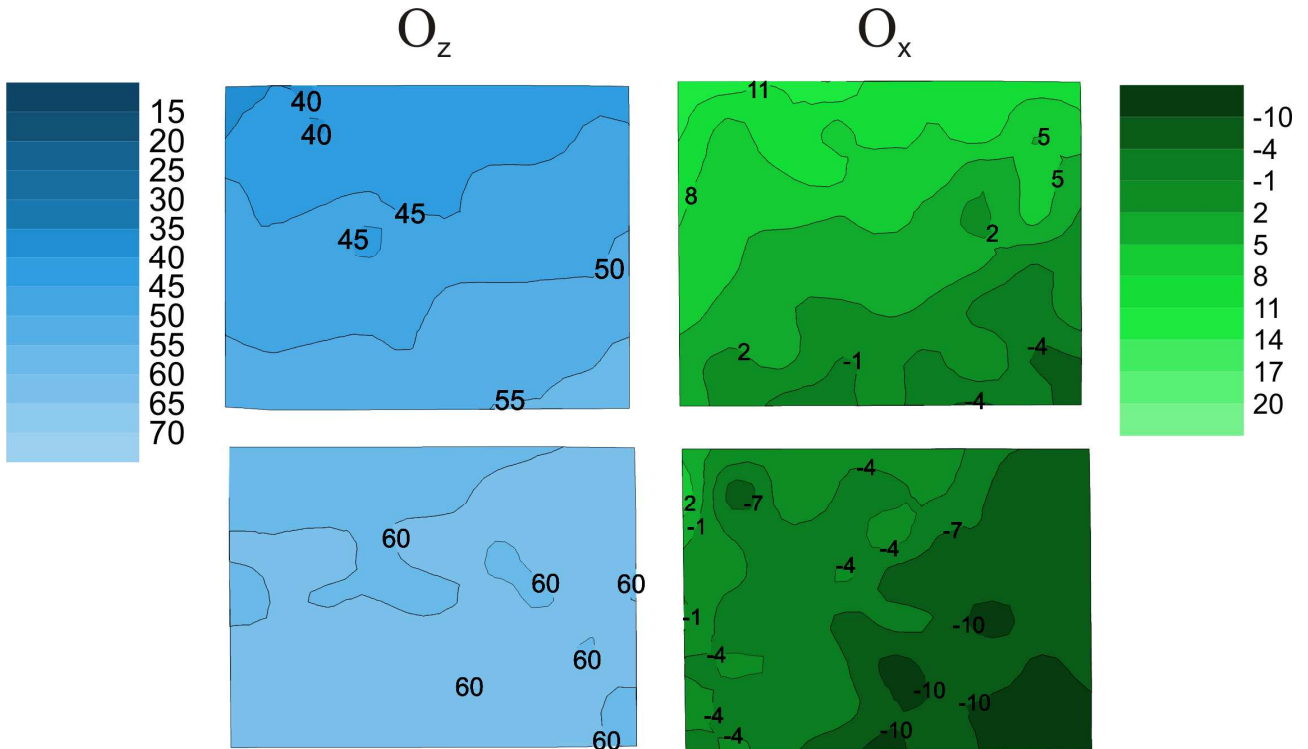


Figure 6. Orientation map of upper and lower sections of Part 1 of HIPS-B. The orientation index,  $O$ , is plotted as percent value for the  $z$  (left) and  $x$  (right) direction, according to the coordinate system indicated in Figure 1.

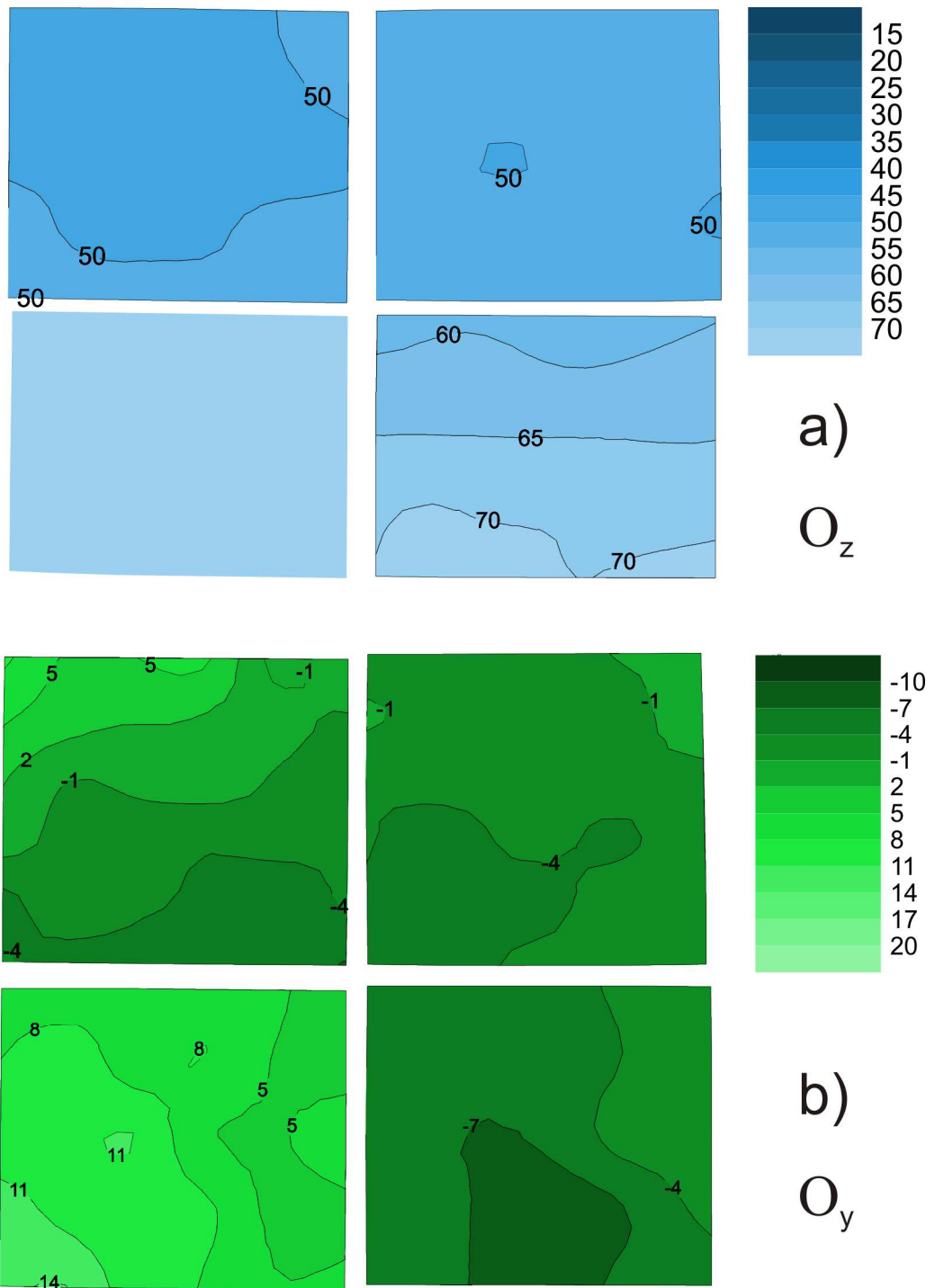


Figure 7. Orientation map of the four sections of Part 2 of HIPS-B. The orientation index,  $O$ , is plotted as percent value for the z (a) and y (b) direction, according to the coordinate system indicated in Figure 1.

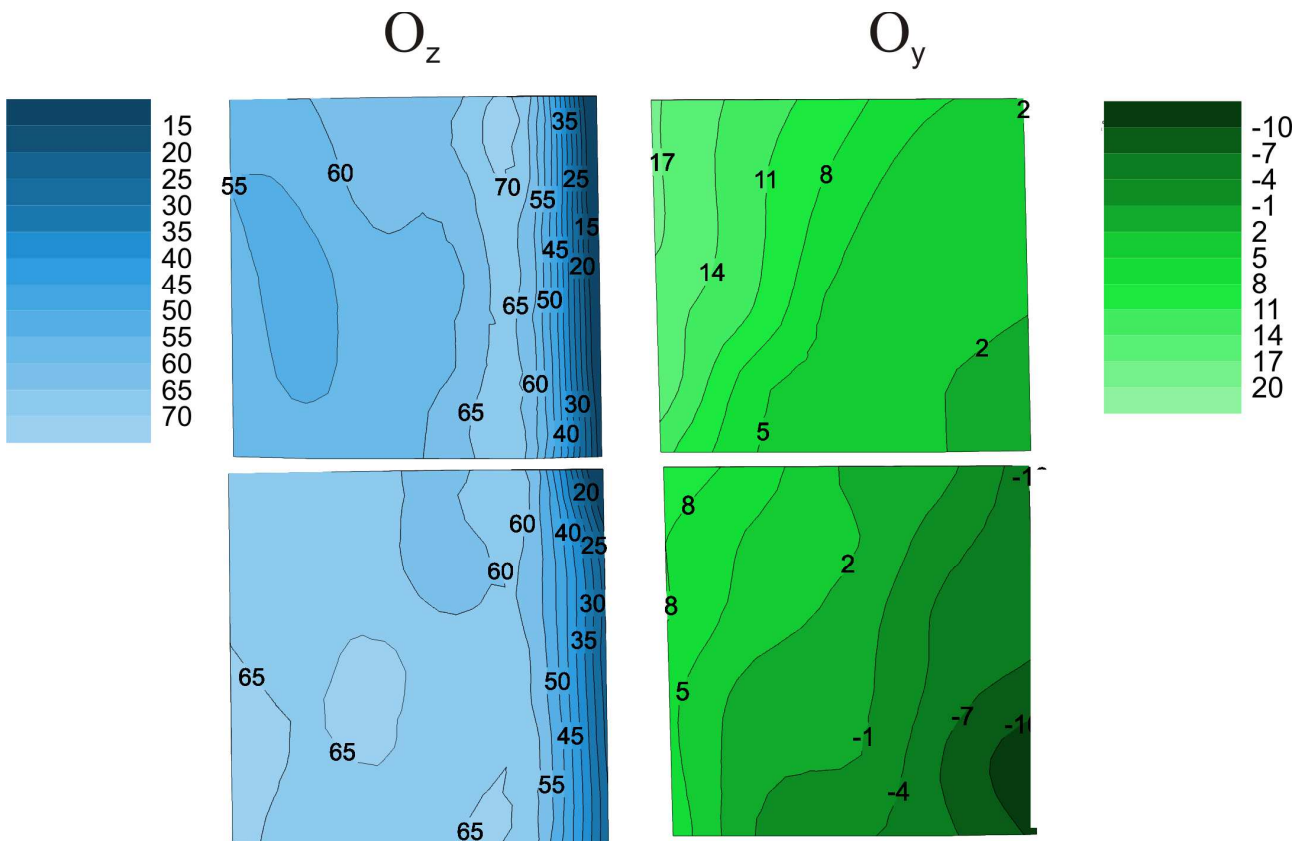


Figure 8. Orientation map of upper and lower sections of Part 3 of HIPS-B. The orientation index,  $O$ , is plotted as percent value for the  $z$  (left) and  $y$  (right) direction, according to the coordinate system indicated in Figure 1.

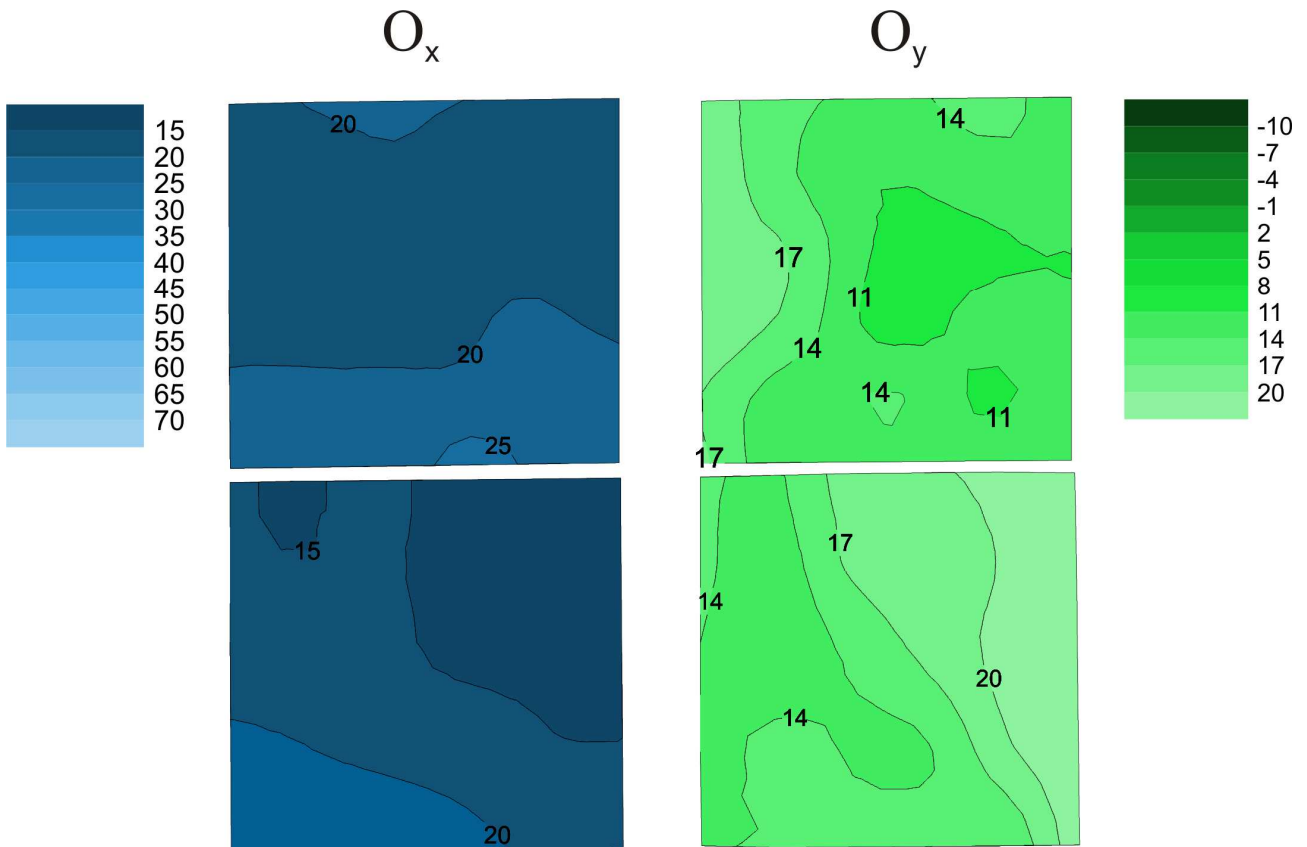


Figure 9. Orientation map of front and back sections of Part 4 of HIPS-B. The orientation index,  $O$ , is plotted as percent value for the x (left) and y (right) direction, according to the coordinate system indicated in Figure 1.

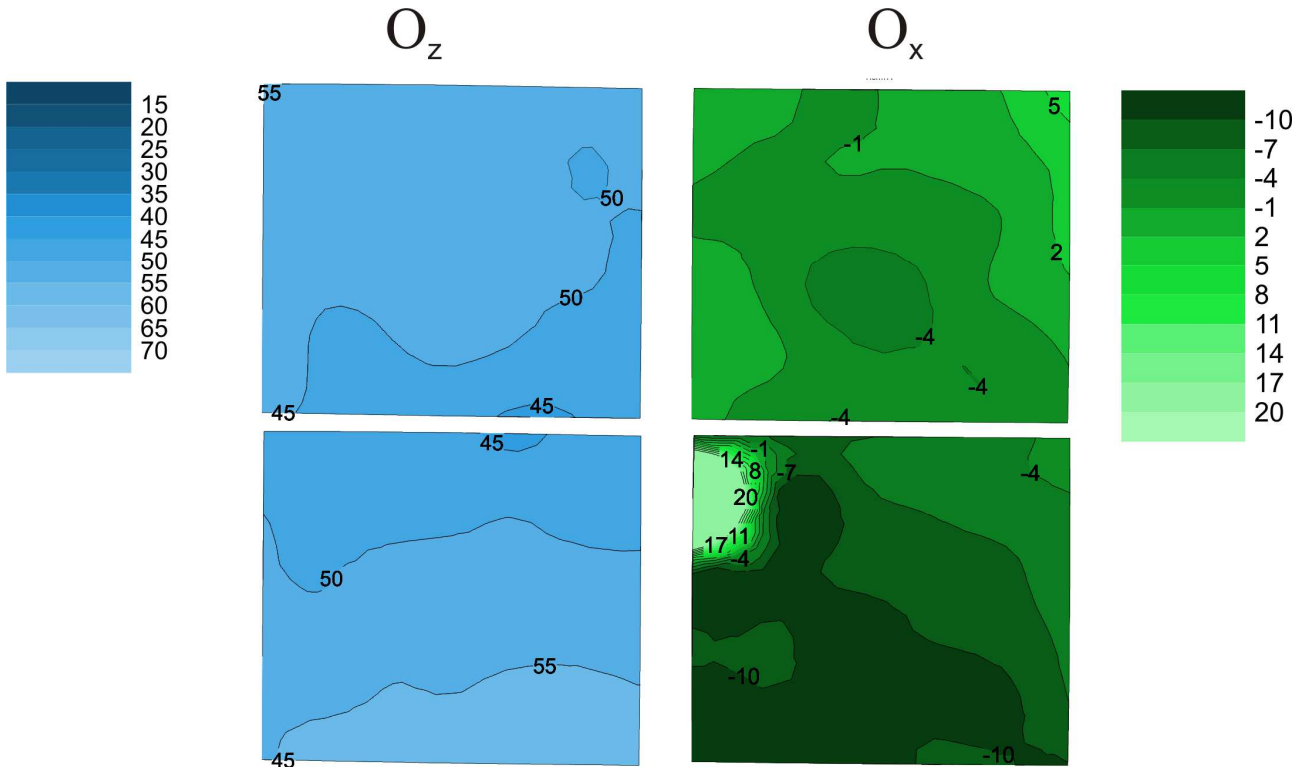


Figure 10. Orientation map of upper and lower sections of Part 5 of HIPS-B. The orientation index,  $O$ , is plotted as percent value for the  $z$  (left) and  $x$  (right) direction, according to the coordinate system indicated in Figure 1.

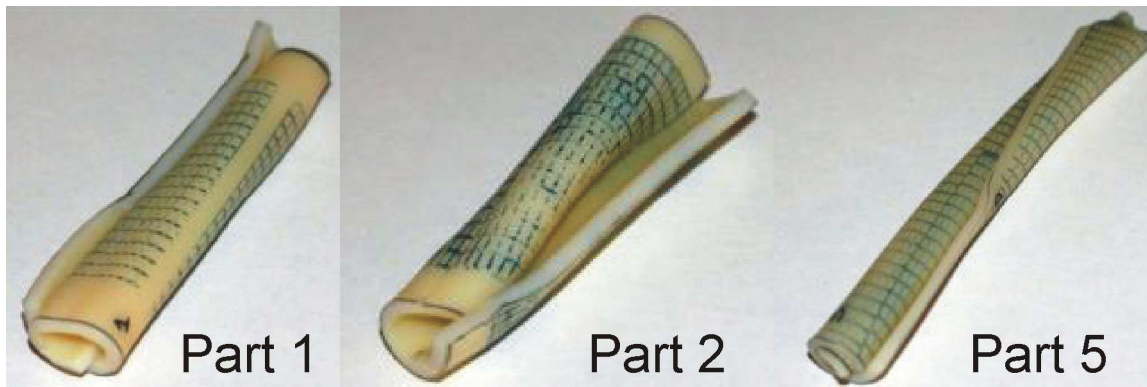


Figure 11. Parts 1, 2 and 5 of thermoformed product made of HIPS-A after thermal treatment at  $T > T_g$ .

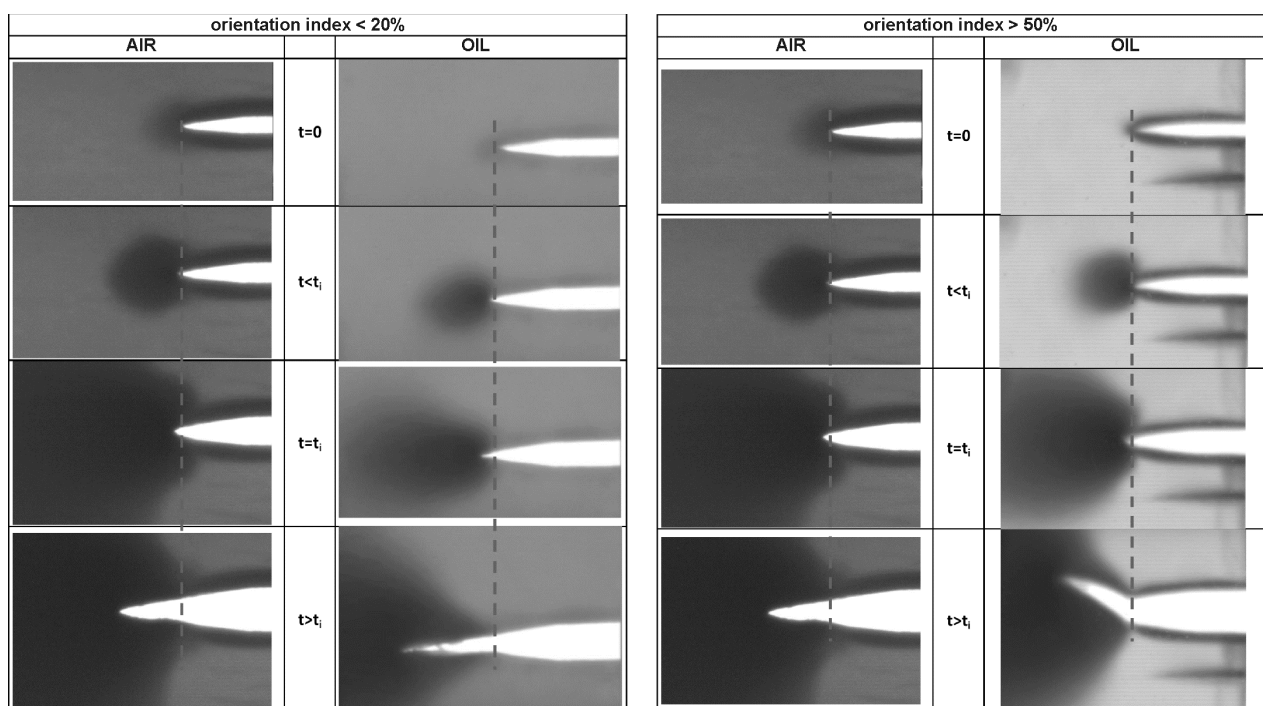


Figure 13. Fracture phenomenology of HIPS-B in air and sunflower oil, respectively for low (left) and high (right) orientation. The sequences of images are taken at different stages during the fracture test: initially and before, at and after the initiation time,  $t_i$ . The dashed lines represent the initial crack tip position.

